SECURITY INFORMATION

Copy
RM L53I03

NACA RM L53I03

TECH LIBRARY KAFB, NM
0144265

7466

NACA

RESEARCH MEMORANDUM

COMPONENT TESTS TO DETERMINE THE AERODYNAMIC CHARACTERISTICS OF AN ALL-MOVABLE 70° DELTA CANARD-TYPE CONTROL IN THE PRESENCE OF A BODY AT A MACH NUMBER OF 1.61

By M. Leroy Spearman

Langley Aeronautical Laboratory
Langley Field, Va.

[redacted] Affecting the National Defense of the United States within the meaning of [redacted] the transmission or revelation of [redacted] in any manner to an unauthorized person is prohibited by law.

NATIONAL ADVISORY COMMITTEE
FOR AERONAUTICS

WASHINGTON

October 9, 1953

Classification cancelled (or changed to UNCLASSIFIED)

By Authority of NSA Tech P.B. Announcement #1
(OFFICER AUTHORIZED TO CHANGE)

By 14 Nov 95
NAME AND

GRADE OF OFFICER MAKING CHANGE)

28 Mar 01
DATE

TECH LIBRARY KAFB, NM
0144265

lU

NATIONAL ADVISORY COMMITTEE FOR AERONAUTICS

RESEARCH MEMORANDUM

COMPONENT TESTS TO DETERMINE THE AERODYNAMIC CHARACTERISTICS OF AN ALL-MOVABLE 70° DELTA CANARD-TYPE CONTROL IN THE PRESENCE OF A BODY AT A MACH NUMBER OF 1.61

By M. Leroy Spearman

SUMMARY

A limited investigation has been conducted in the Langley 4- by 4-foot supersonic pressure tunnel to determine the aerodynamic characteristics of a body-control arrangement at a Mach number of 1.61. A 70° delta canard-type control mounted in the horizontal plane and having a span-to-body-diameter ratio at the control trailing edge of 2.52 was tested both fixed and moving in the presence of a long cylindrical body (fineness ratio of 19.1) with a parabolic nose. Some limited tests were made with vertical canards installed and some with nacelles mounted in the vertical plane on unswept pylons near the rear of the body.

The lift, pitching-moment, and control hinge-moment characteristics were compared with estimated characteristics at a Mach number of 1.61 for the body-canard arrangement.

The effect of sideslip was such that the lift effectiveness of the pitch control increased as the sideslip angle increased. Deflection of the pitch control in sideslip had a large effect on the induced roll of the model with nacelles in that the variation of rolling-moment coefficient with sideslip angle changed from a positive slope to a negative slope as the control deflection was varied from negative to positive.

INTRODUCTION

Low-aspect-ratio, all-movable wings or control surfaces have become increasingly important as a means of control at supersonic speeds, particularly for canard-type missiles. Some experimental results such as those presented in references 1 and 2 are available for such body and

[redacted]

control arrangements, but these investigations are concerned only with lift, drag, and pitching-moment characteristics. A limited amount of data concerning the rolling-moment variation with sideslip for a variable-incidence wing mounted on a body are presented in reference 3.

The present investigation provides six-component results as well as some control hinge-moment results at a Mach number of 1.61 for various configurations including a fineness-ratio-19.1 body alone, a body with 70° delta canard-type controls, and a body with controls and with pylon-mounted nacelles in the vertical plane near the rear of the body. These results should be useful in providing an experimental insight into similar body-control designs and should also provide additional experimental results that may be correlated with theoretical studies, such as those presented in references 4 to 7.

Tests were made through a body angle-of-attack range from -4° to 10° at zero sideslip and through a sideslip range from -4° to 10° at zero angle of attack. Deflections of the horizontal control ranged from -6° to 12° and deflections of the vertical control were 0° and 6°.

COEFFICIENTS AND SYMBOLS

The results of the tests are presented as standard NACA coefficients of forces and moments. The data are referred to the stability-axes system (fig. 1) with the reference center of gravity at body station 34.167 (fig. 2). The coefficients and symbols are defined as follows:

C_L lift coefficient, $-Z/qS$

C_D drag coefficient, $-X/qS$

C_Y lateral-force coefficient, Y/qS

C_l rolling-moment coefficient, L/qSb

C_m pitching-moment coefficient, $M'/qS\bar{c}$

C_n yawing-moment coefficient, N/qSb

C_h control hinge-moment coefficient, $H/qS\bar{c}$

C_{L_F} lift coefficient for body alone, $-Z/qF$

C_{D_F}	drag coefficient for body alone, $-X/qF$
C_{m_F}	pitching-moment coefficient for body alone, M'/qFl
X	force along X-axis
Y	force along Y-axis
Z	force along Z-axis
L	moment about X-axis
M'	moment about Y-axis
N	moment about Z-axis
H	moment about control hinge axis
q	free-stream dynamic pressure
S	exposed area of horizontal control
b	total span of control including body
$\bar{c}$	mean aerodynamic chord for exposed control
F	body base area
l	body length
M	Mach number
L/D	lift-drag ratio, C_L/C_D
α	angle of attack of body, deg
α'	angle of attack of horizontal control, $\alpha + \delta_H$, deg
δ_H	deflection of horizontal control with respect to body axis, deg
δ_V	deflection of vertical control with respect to body axis, deg
β	angle of sideslip, deg

$C_{L_{\alpha'}}$ $\left(\frac{dC_L}{d\alpha'}\right)_{\delta_H}$

$C_{m_{\alpha'}}$ $\left(\frac{dC_m}{d\alpha'}\right)_{\delta_H}$

$C_{L_{\delta_H}}$ $\left(\frac{dC_L}{d\delta_H}\right)_{\alpha}$ or $\left(\frac{dC_L}{d\alpha'}\right)_{\alpha}$

$C_{m_{\delta_H}}$ $\left(\frac{dC_m}{d\delta_H}\right)_{\alpha}$ or $\left(\frac{dC_m}{d\alpha'}\right)_{\alpha}$

C_{Y_β} $\left(\frac{dC_Y}{d\beta}\right)$

C_{n_β} $\left(\frac{dC_n}{d\beta}\right)$

C_{l_β} $\left(\frac{dC_l}{d\beta}\right)$

$C_{h_{\alpha'}}$ $\left(\frac{dC_h}{d\alpha'}\right)_{\delta_H}$

$C_{h_{\delta_H}}$ $\left(\frac{dC_h}{d\delta_H}\right)_{\alpha}$ or $\left(\frac{dC_h}{d\alpha'}\right)_{\alpha}$

The subscripts outside the parentheses represent the factors held constant during the measurement of the parameters.

MODEL AND APPARATUS

Details of the model are shown in figure 2 and the geometric characteristics of the model are presented in table I.

The body had a fineness ratio of 19.1 and was composed of a parabolic nose followed by a frustrum of a cone which was faired into a cylinder. Coordinates for the body are given in table II. The control surfaces which were mounted on the conical section of the body had hexagonal sections and delta plan forms with 70° swept leading edges and were deflected about an axis normal to the body center line. The vertical canard had approximately half the area of the horizontal canard (see fig. 3) and the resulting ratios of control span to body diameters at the control trailing edge were 2.07 and 2.52. The horizontal canard tapered in thickness toward the tip and had a constant thickness ratio of about 0.041. The vertical canard had a constant thickness with a thickness ratio of about 0.058 at the root. The nacelles (fig. 2) were mounted in the angle-of-attack plane on unswept pylons near the rear of the body.

Force measurements were made through the use of a six-component internal strain-gage balance. An individual strain-gage balance was used to measure the hinge moment for the horizontal control.

TESTS

Tests were made through a body angle-of-attack range from -4° to 10° at zero sideslip and through a sideslip range from -4° to 10° at zero angle of attack. Deflections of the horizontal control ranged from -6° to 12° and deflections of the vertical control were 0° and 6°.

The test conditions are given as follows:

Mach number	1.61
Reynolds number based on large control M.A.C.	0.88×10^6
Reynolds number based on small control M.A.C.	0.62×10^6
Stagnation pressure, atm	1.0
Stagnation temperature, °F	110

The stagnation dewpoint was sufficiently low (less than -25° F) so that no condensation effects were encountered in the test section.

CORRECTIONS AND ACCURACY

The angles of attack and sideslip were corrected for the deflection of the balance and sting under load. The Mach number variation in the test section was approximately ±0.01 and the flow-angle variation in the

vertical and horizontal planes was approximately $\pm 0.1^{\circ}$. No corrections were applied to the data to account for these flow variations.

The maximum estimated errors in the individual measured quantities are given as follows:

	Large control	Body
C_L	±0.062	±0.072
C_D	±.034	±.041
C_m	±.028	±.0016
C_Y	±.016	
C_n	±.017	
C_l	±.014	
C_h	±.0005	

The angles of attack and sideslip and the control deflection angles are accurate to within $\pm 0.1^{\circ}$. The base pressure was measured and the drag data were corrected to a base pressure equal to the free-stream static pressure. Errors in the base-pressure measurements are included in the estimated error of C_D.

RESULTS AND DISCUSSION

Presentation of Data

Results are presented for four variations of the test model: (1) body alone, (2) body with large horizontal canard-type control, (3) body with large horizontal and small vertical canard-type controls, and (4) body with horizontal and vertical controls with pylon-mounted nacelles in the vertical plane near the rear of the model.

A table of the figures presenting the results is given as follows:

Some experimental and theoretical results are presented in table III.

Effect of Angle of Attack

The lift, drag, and pitching-moment variations with angle of attack for the body alone (fig. 4) are compared with the theoretical variations obtained by the method of reference 8. The change in drag with angle of attack indicated by the method of reference 8 was applied to the experimental minimum drag value.

The characteristics of the body with the horizontal control both fixed to the body at zero deflection and as an all-moving surface in the presence of the body are presented (fig. 5) as a function of the control-surface angle of attack which is the body angle of attack plus the control deflection angle. Hence, the results for the all-movable control at constant body angles correspond to the usual control parameters. For example, in the case of lift, $C_{L_{\alpha'}}$ with the body angle constant corresponds to $C_{L_{\delta_H}}$ for the control.

[redacted]

The theoretical variation of C_L with α' for the small angle range was obtained for the body-control fixed through the use of reference 5. These results were combined with the theoretical results obtained for the body alone (ref. 8) to determine approximately the shape of the body-control fixed curve at the higher angles. This method considers only the deviation from linearity indicated by the estimated body-alone results.

The theoretical variation of C_L with α' for the all-moving control with the body at zero angle of incidence was obtained through the use of reference 9 for an isolated delta-plan-form surface. The agreement of the theoretically determined slopes with the experimentally determined slopes indicates that there is no effect of the body on the control lift.

Theoretical hinge-moment characteristics for the control were also obtained from reference 9 for an isolated delta plan form. These results are in closer agreement with the experimental body-control fixed results than with the all-moving-control results, even for a body angle of attack of zero. Inasmuch as the method of reference 9 shows good agreement with experimental results for the all-moving-control lift but not for the all-moving-control moment, the indication is that the gap between the deflected control and the body, although not appreciably affecting the control lift, does result in a more forward location of the control center of pressure. Such an effect, although contrary to what might be expected, was also observed in the investigations reported in references 1 and 2.

The theoretical center-of-pressure location for the body control fixed obtained by the method of reference 6 was used to determine the theoretical variation of C_m with α' (fig. 5). This result was combined with the body-alone theoretical results in the same manner as for the lift curves in order to determine the shape of the curve at the higher angles. The theoretical curve for the all-moving control case at a body angle of 0° was obtained by converting the theoretical value of $C_{L_{\alpha'}}$ to $C_{m_{\alpha'}}$ through the relation $C_{m_{\alpha'}} = C_{L_{\alpha'}}\frac{x}{c}$ where x is the distance between the model center of gravity and the 2/3 root chord of the horizontal control.

The Effect of Sideslip

The effect of β on the horizontal control characteristics at $\alpha = 0$ (fig. 6) is manifest primarily as an increase in $C_{L_{\delta_H}}$ at $\beta = 10^\circ$ with little change in $C_{m_{\delta_H}}$ or $C_{h_{\delta_H}}$. The lateral characteristics indicate

an increase in the negative values of C_{Y_β} and C_{n_β} with increasing δ_H and a change in C_{l_β} from positive to negative as δ_H is varied from negative to positive. These lateral characteristics are also shown in figure 7 where the variation of C_Y, C_l, and C_n with β is shown for various control deflections.

The variations of the lateral characteristics with δ_H for the model with both a horizontal and a vertical-control surface for δ_V of 0° and 6° (fig. 8) are similar to those for the model without the vertical control.

The effect of δ_H on the aerodynamic characteristics in sideslip of the model with horizontal and vertical controls and with nacelles mounted in the vertical plane near the rear of the body is presented in figure 9 for vertical control deflections of 0° and 6°. The results are similar to those shown previously for the body with controls in that a large increase in $C_{L_{\delta_H}}$ with increasing β is indicated. However, much larger changes in C_{l_β} with δ_H are indicated, apparently a result of the control-surface flow field acting on the nacelle and pylon. These changes in C_{l_β} indicate a positive dihedral effect with positive δ_H and negative dihedral effect with negative δ_H. The addition of the nacelles, of course, causes a large stabilizing yawing moment and a large increase in the lateral force.

CONCLUDING REMARKS

The results of an investigation made at a Mach number of 1.61 to determine the aerodynamic characteristics of a canard-type body-control arrangement indicated a pronounced effect of sideslip on the pitch-control characteristics in that the lift effectiveness of the pitch control increased considerably as the sideslip angle increased. In addition, deflection of the pitch control caused large changes in the rolling moment due to sideslip for the model with canard controls and pylon-mounted nacelles in the vertical plane near the rear of the body. These

changes were such that the rolling moment due to sideslip changed from positive to negative as the pitch-control deflection was changed from negative to positive.

Langley Aeronatuical Laboratory,
National Advisory Committee for Aeronautics,
Langley Field, Va., August 20, 1953.

[redacted]

REFERENCES

1. Conner, D. William: Aerodynamic Characteristics of Two All-Movable Wings Tested in the Presence of a Fuselage at a Mach Number of 1.9. NACA RM L8H04, 1948.

2. Stivers, Louis S., Jr., and Malick, Alexander W.: Wind-Tunnel Investigation at Mach Numbers From 0.50 to 1.29 of an All-Movable Triangular Wing of Aspect Ratio 4 Alone and With a Body. NACA RM A9L01, 1950.

3. Scherrer, Richard, and Dennis, David H.: Lateral-Control Characteristics and Dihedral Effect of a Wing-Body Combination With a Variable-Incidence Triangular Wing and Wing-Tip Ailerons at a Mach Number of 1.52. NACA RM A50H10, 1951.

4. Nielsen, Jack N., Katzen, Elliott D., and Tang, Kenneth K.: Lift and Pitching-Moment Interference Between a Pointed Cylindrical Body and Triangular Wings of Various Aspect Ratios at Mach Numbers of 1.50 and 2.02. NACA RM A50F06, 1950.

5. Nielsen, Jack N., and Kaattari, George E.: Method for Estimating Lift Interference of Wing-Body Combinations at Supersonic Speeds. NACA RM A51J04, 1951.

6. Kaattari, George E., Nielsen, Jack N., and Pitts, William C.: Method for Estimating Pitching-Moment Interference of Wing-Body Combinations at Supersonic Speeds. NACA RM A52B06, 1952.

7. Nielsen, Jack N., Kaattari, George E., and Drake, William C.: Comparison Between Prediction and Experiment for All-Movable Wing and Body Combinations at Supersonic Speeds - Lift, Pitching Moment, and Hinge Moment. NACA RM A52D29, 1952.

8. Allen, H. Julian: Estimation of the Forces and Moments Acting on Inclined Bodies of Revolution of High Fineness Ratio. NACA RM A9I26, 1949.

9. Ribner, Herbert S., and Malvestuto, Frank S., Jr.: Stability Derivatives of Triangular Wings at Supersonic Speeds. NACA Rep. 908, 1948. (Supersedes NACA TN 1572.)

TABLE I.- GEOMETRIC CHARACTERISTICS OF MODEL

Body:	
Maximum diameter, in.	2.666
Length, in.	50.833
Fineness ratio	19.067
Base area, sq in.	5.583
Horizontal canard:	
Area (exposed), sq in.	6.406
Aspect ratio	1.73
Sweep angle of leading edge, deg	70
Mean aerodynamic chord, in.	2.576
Span-to-body-diameter ratio	2.52
Vertical canard:	
Area (exposed), sq in.	2.94
Aspect ratio	1.73
Sweep angle of leading edge, deg	70
Mean aerodynamic chord, in.	1.821
Span-to-body-diameter ratio	2.07

TABLE II.- BODY COORDINATES

Body station, in.	Radius, in.
0	0
.297	.076
.627	.156
.956	.233
1.285	.307
1.615	.378
1.945	.445
2.275	.509
2.605	.573
2.936	.627
3.267	.682
3.598	.732
3.929	.780
4.260	.824
4.592	.865
4.923	.903
5.255	.940
5.587	.968
5.920	.996
6.252	1.020
6.583	1.042
11.542	1.333
50.833	1.333

TABLE III.- AERODYNAMIC PARAMETERS FOR SMALL ANGLE RANGE

Item	Configuration			
	Body with large control		Body alone	
	Experiment	Theory	Experiment	Theory
$C_{L_{\alpha'}}$	0.106	0.084 (ref. 5)	0.054	0.056
$C_{L_{\delta_H}}$	.034	.034 (ref. 9)		
Center-of-pressure location	.225	.167 (ref. 6) .155 (ref. 4)	.021	.024
$C_{m_{\alpha'}}$	1.0	.831 (ref. 6) .86 (ref. 4)		
$C_{m_{\delta_H}}$	.37	.33 (ref. 9)		
$C_{h_{\alpha'}}$	-.0023	-.0026 (ref. 9)		
$C_{h_{\delta_H}}$	-.0017	-.0026 (ref. 9)		

NACA

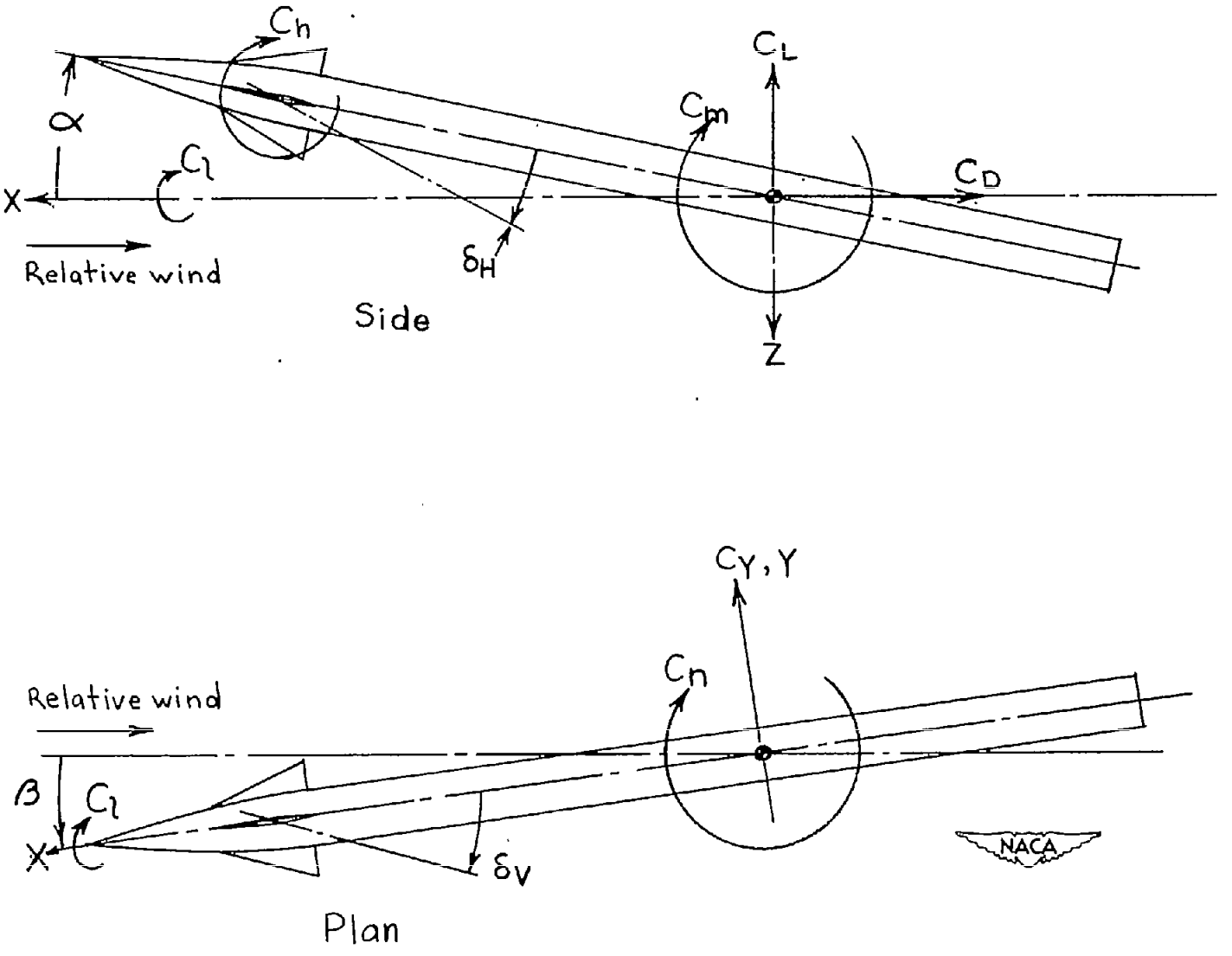

Figure 1.- System of stability axes. Arrows indicate positive values.

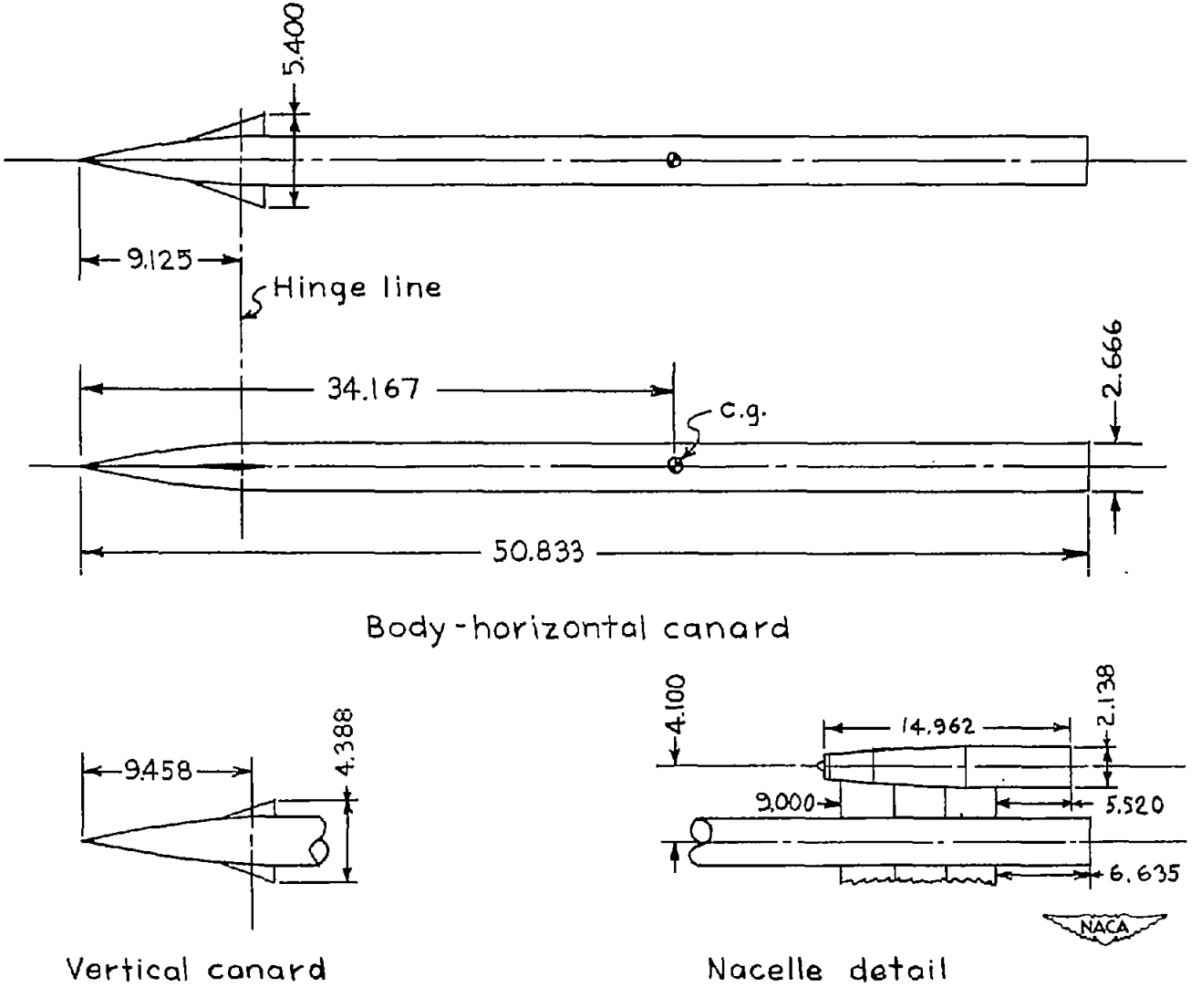

Figure 2.- Details of model. All dimensions are in inches.

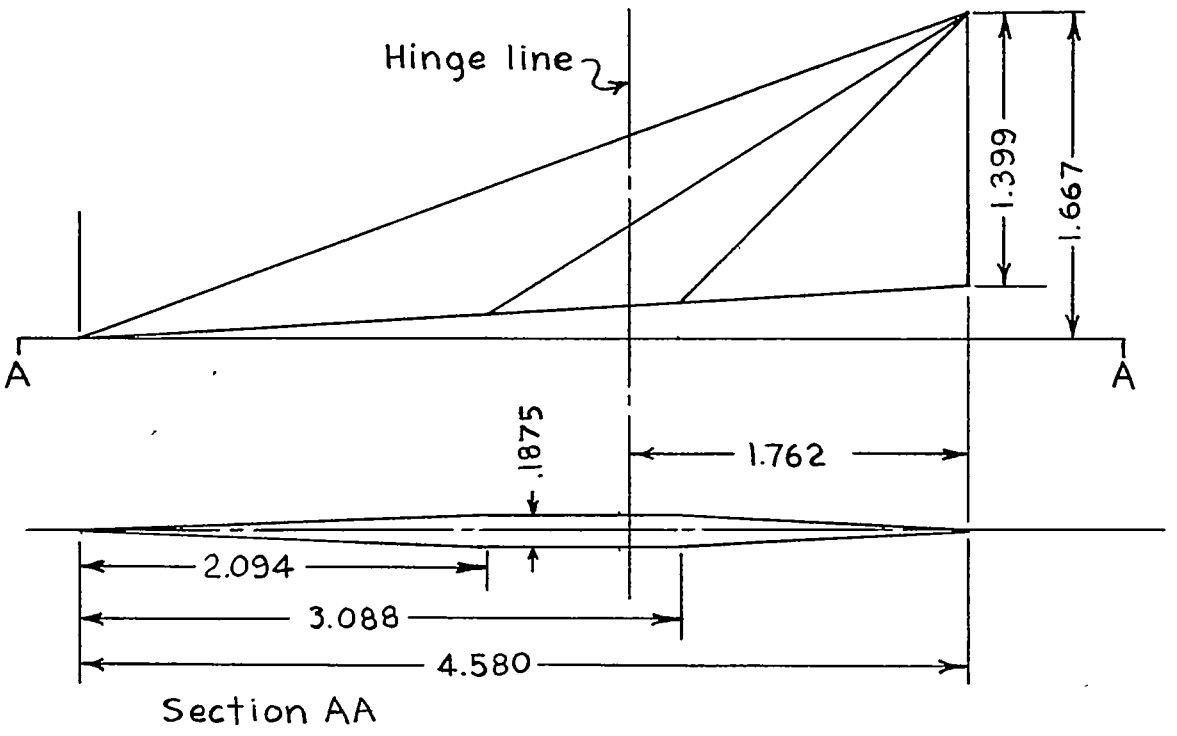

Horizontal canard

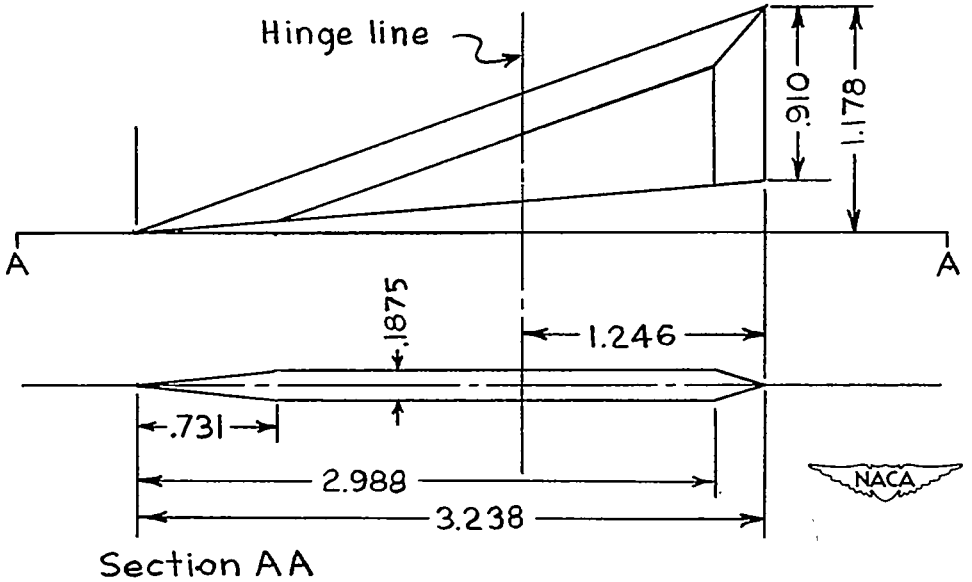

Vertical canard

Figure 3.- Details of canard control surfaces. All dimensions are in inches.

[redacted]

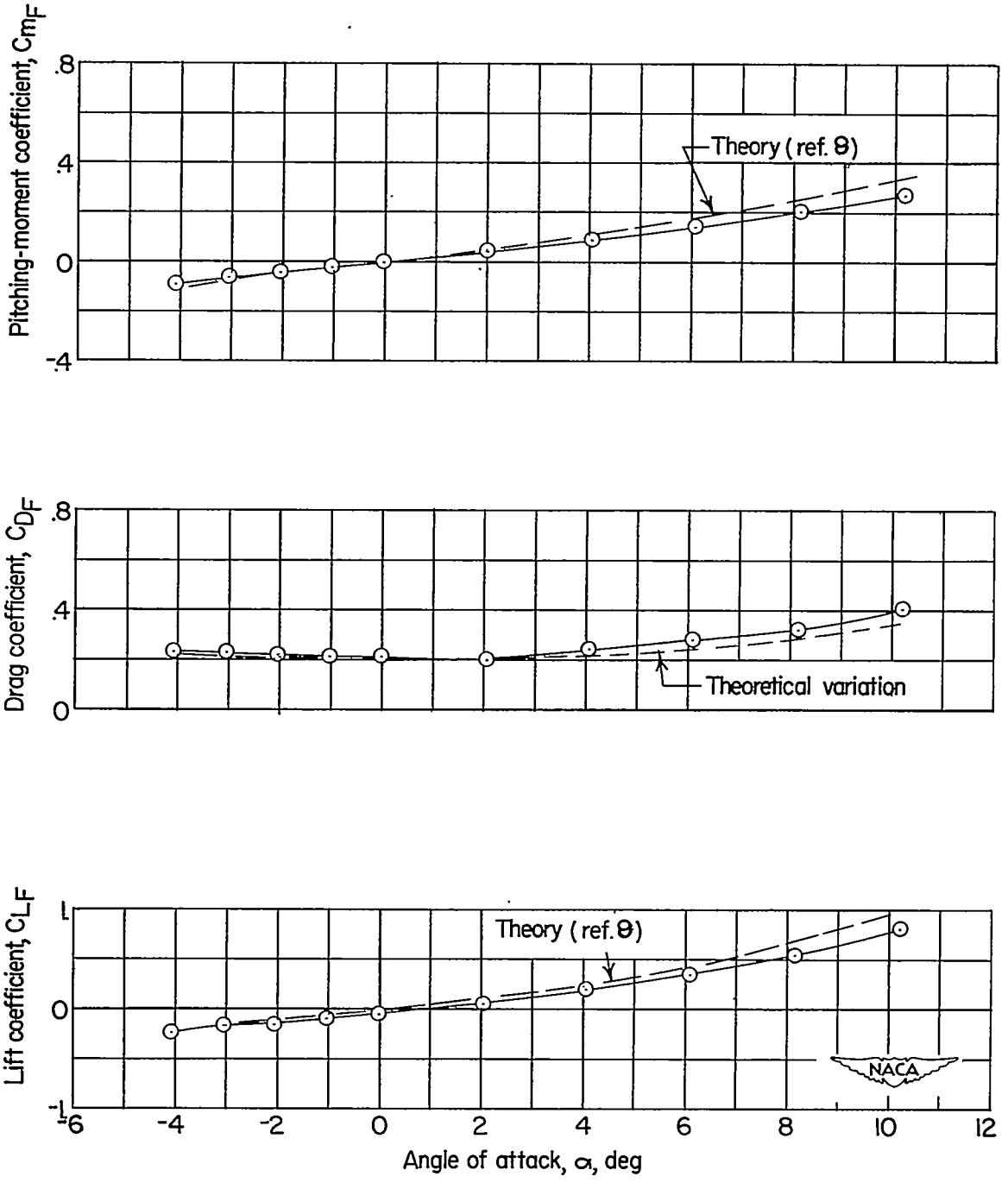

Figure 4.- Aerodynamic characteristics in pitch of the body alone.

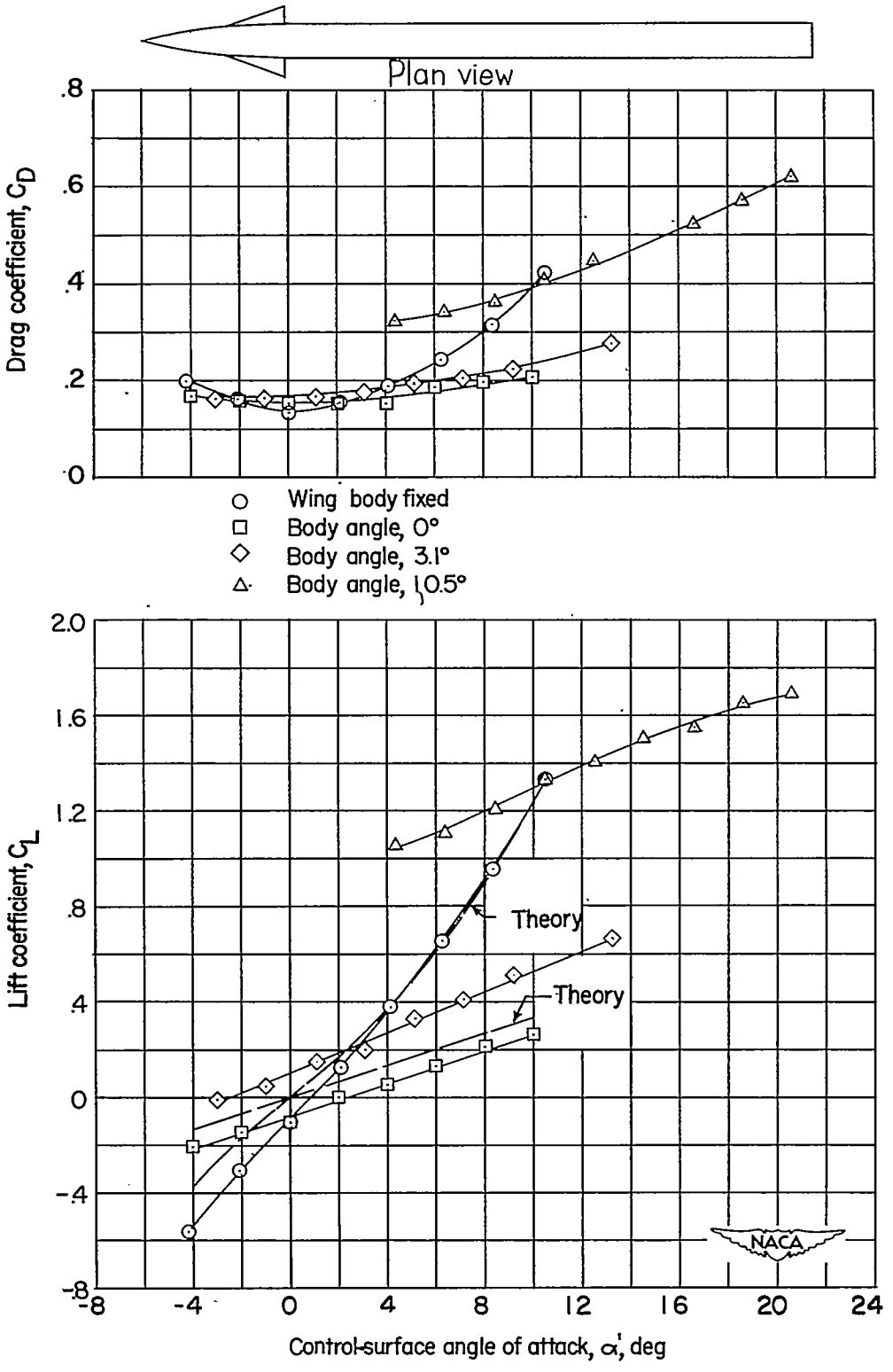

Figure 5.- Aerodynamic characteristics in pitch for body with horizontal canard both fixed and moving.

[redacted]

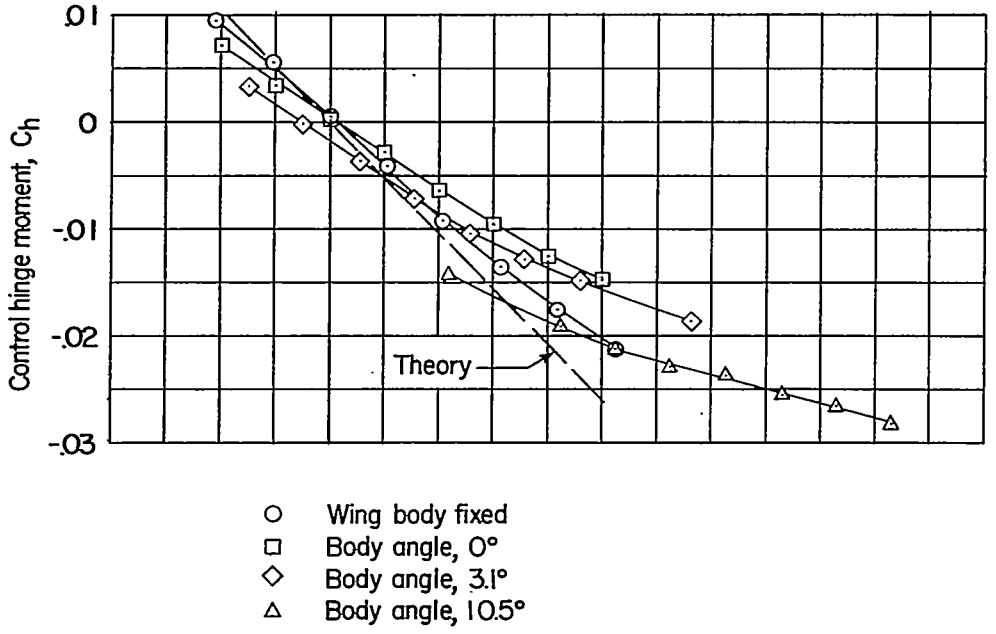

○ Wing body fixed
□ Body angle, 0°
◇ Body angle, 3.1°
△ Body angle, 10.5°

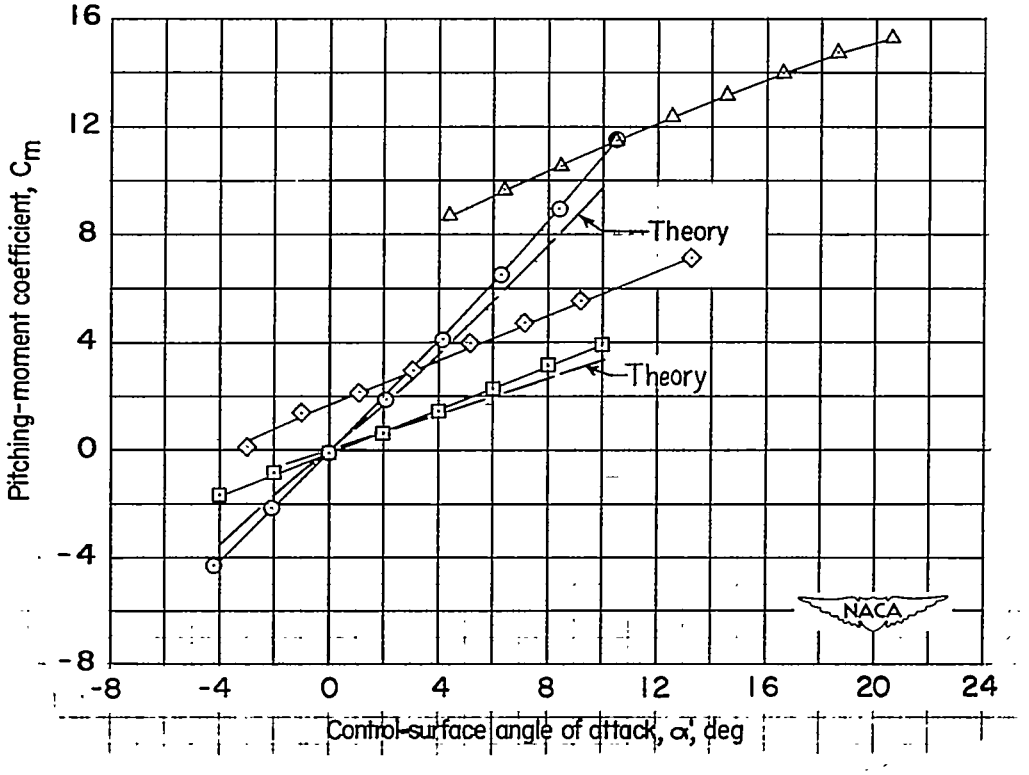

Figure 5.- Continued.

[redacted]

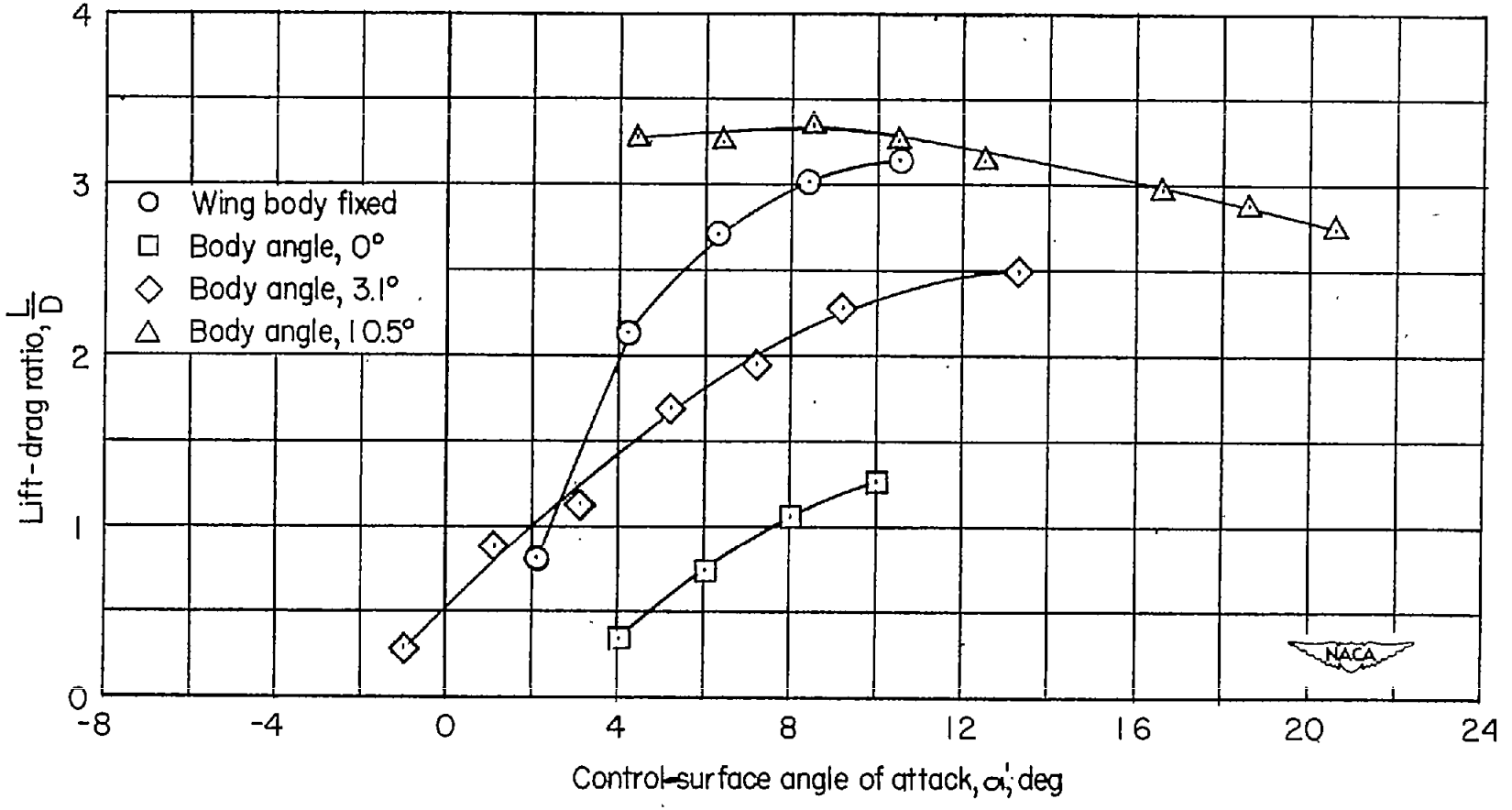

Figure 5.- Concluded.

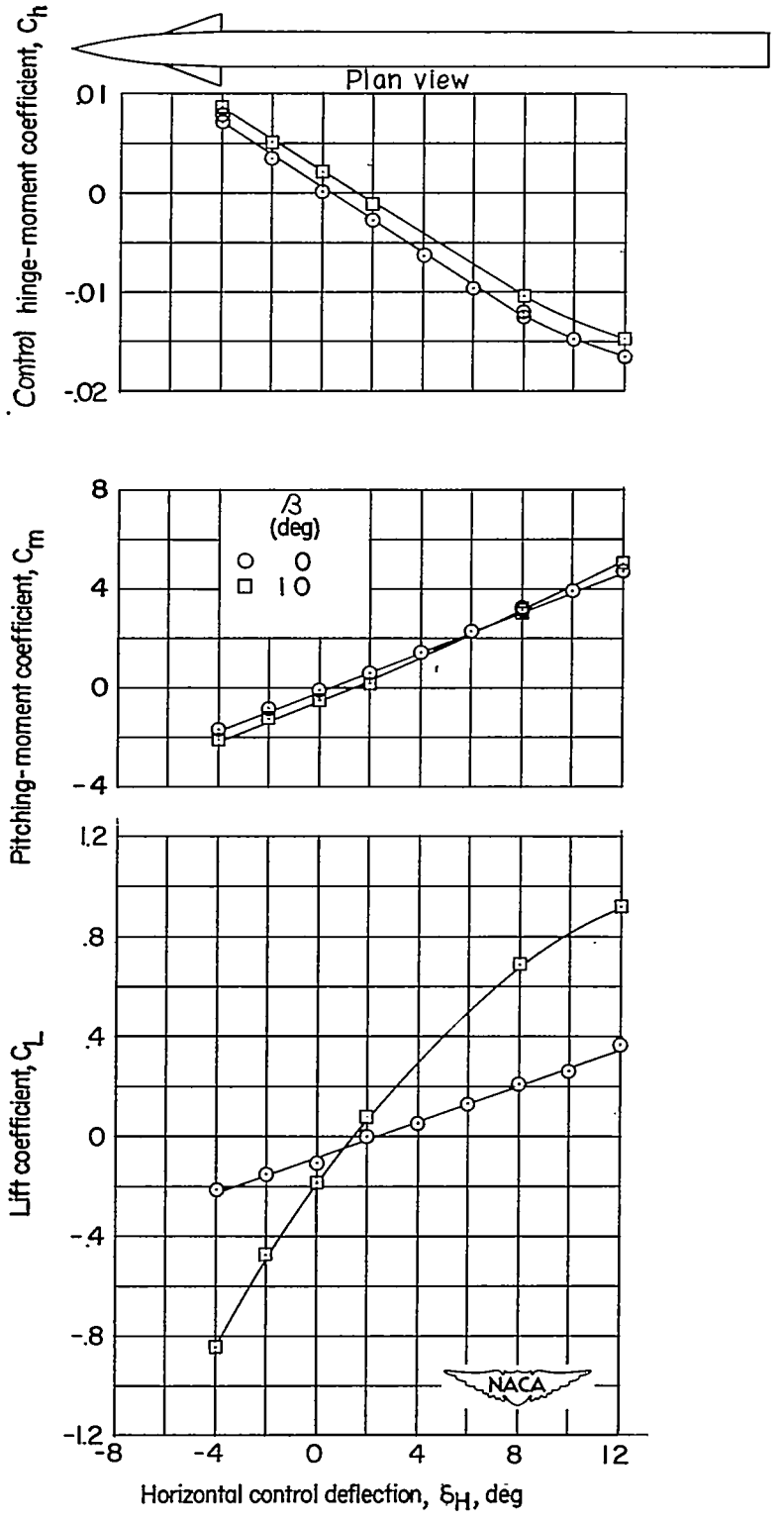

Figure 6.- Effect of sideslip on control characteristics of body with horizontal canard. $\alpha = 0^\circ$.

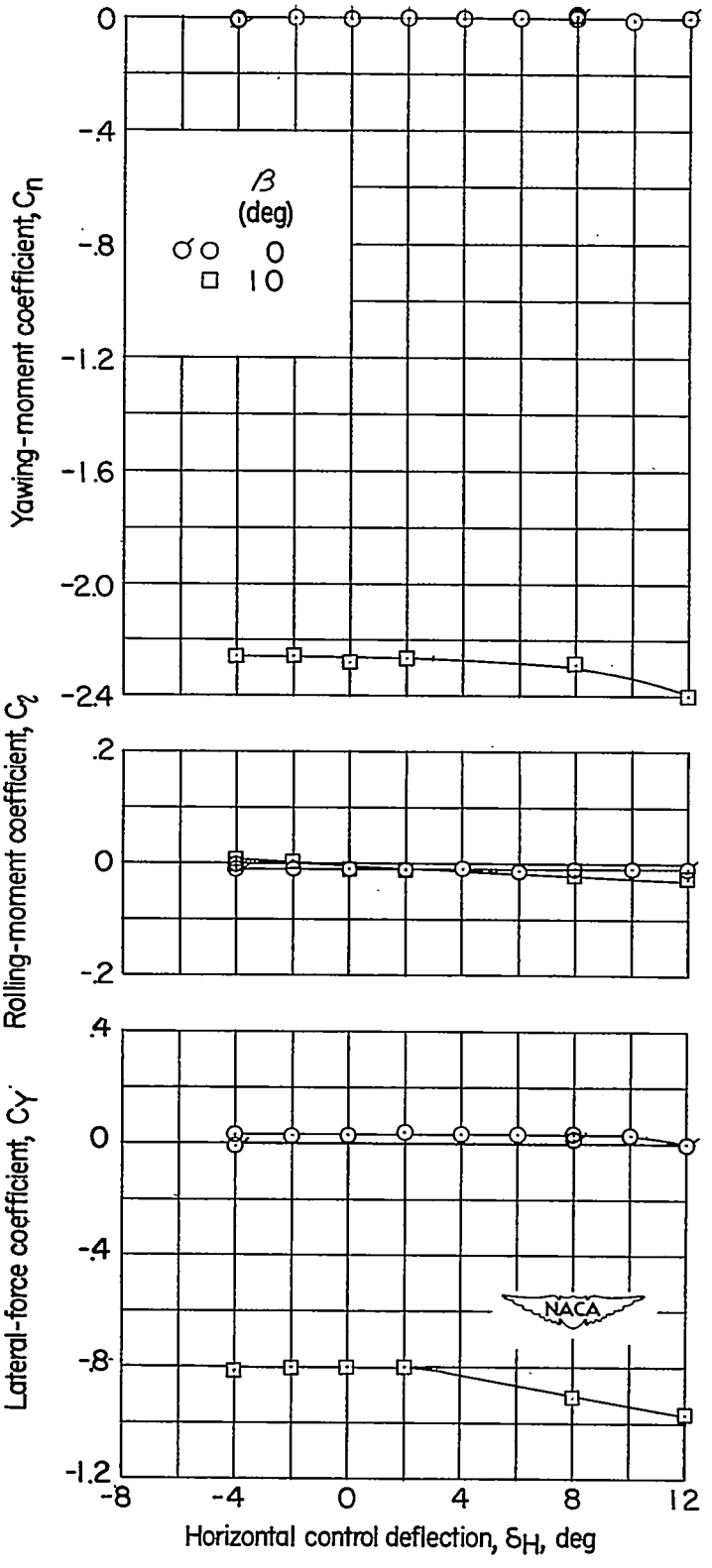

Figure 6.- Concluded.

[redacted]

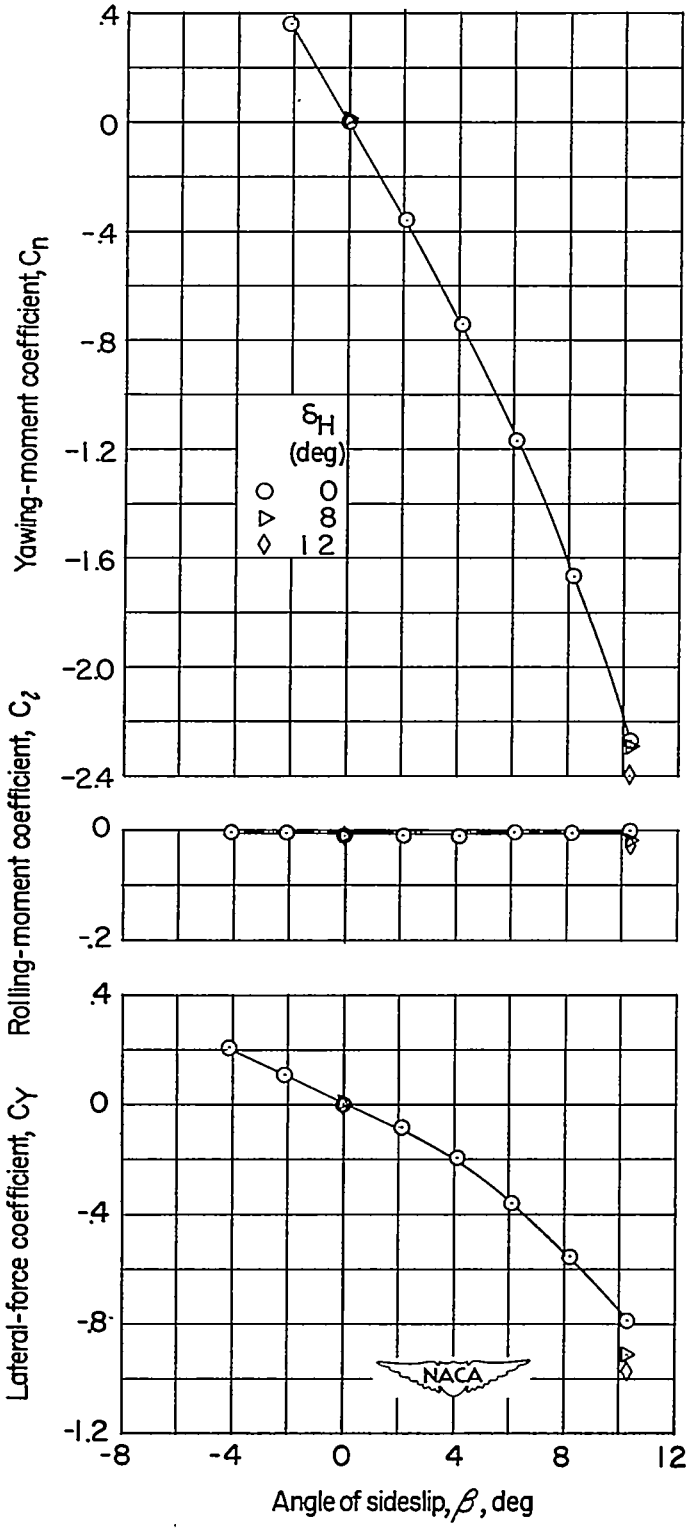

Figure 7.- Aerodynamic characteristics in sideslip for body with horizontal canard.

[redacted]

Figure 8.- Effect of sideslip on control characteristics of body with horizontal and vertical canard.

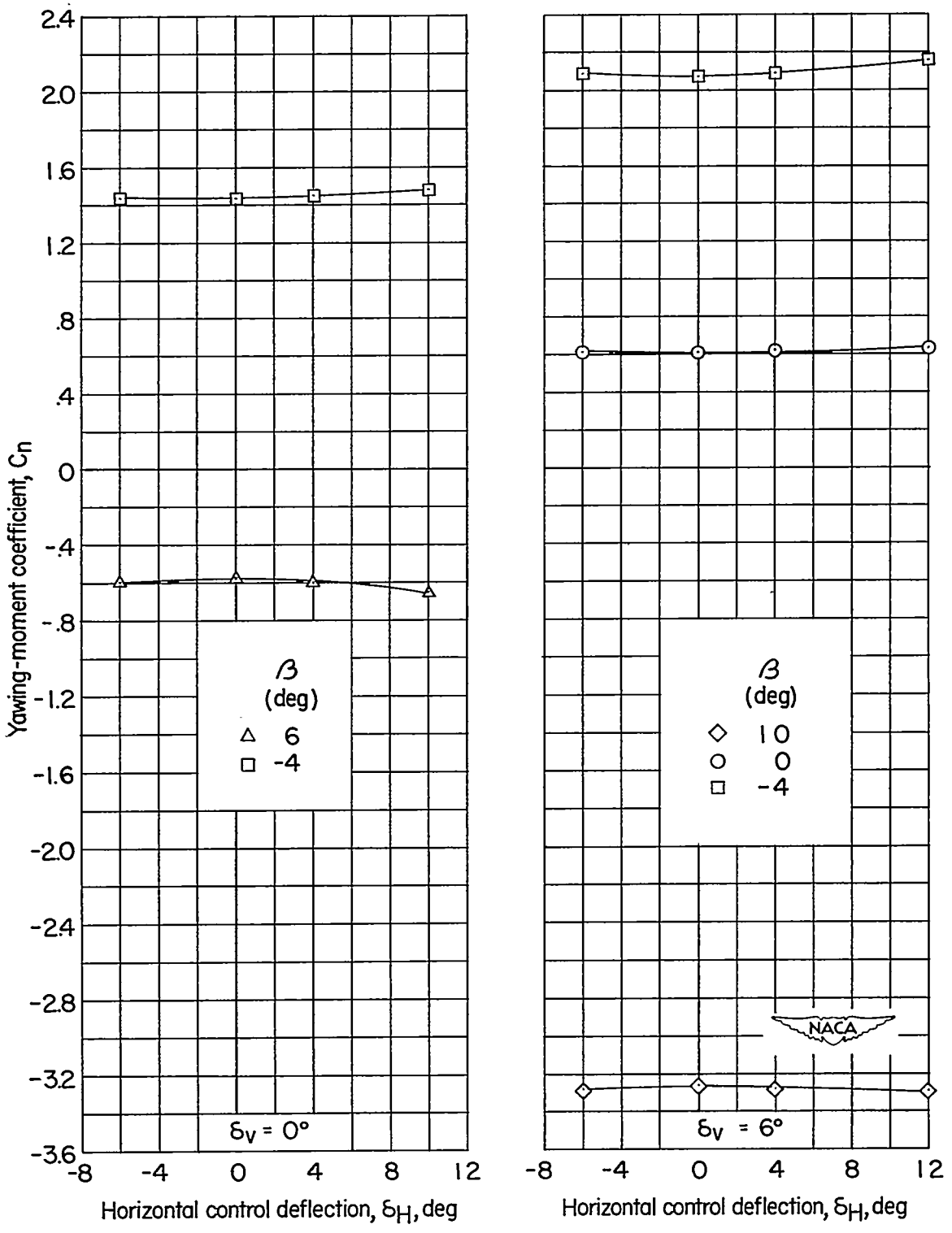

Figure 8.- Concluded.

CONFIDENTIAL

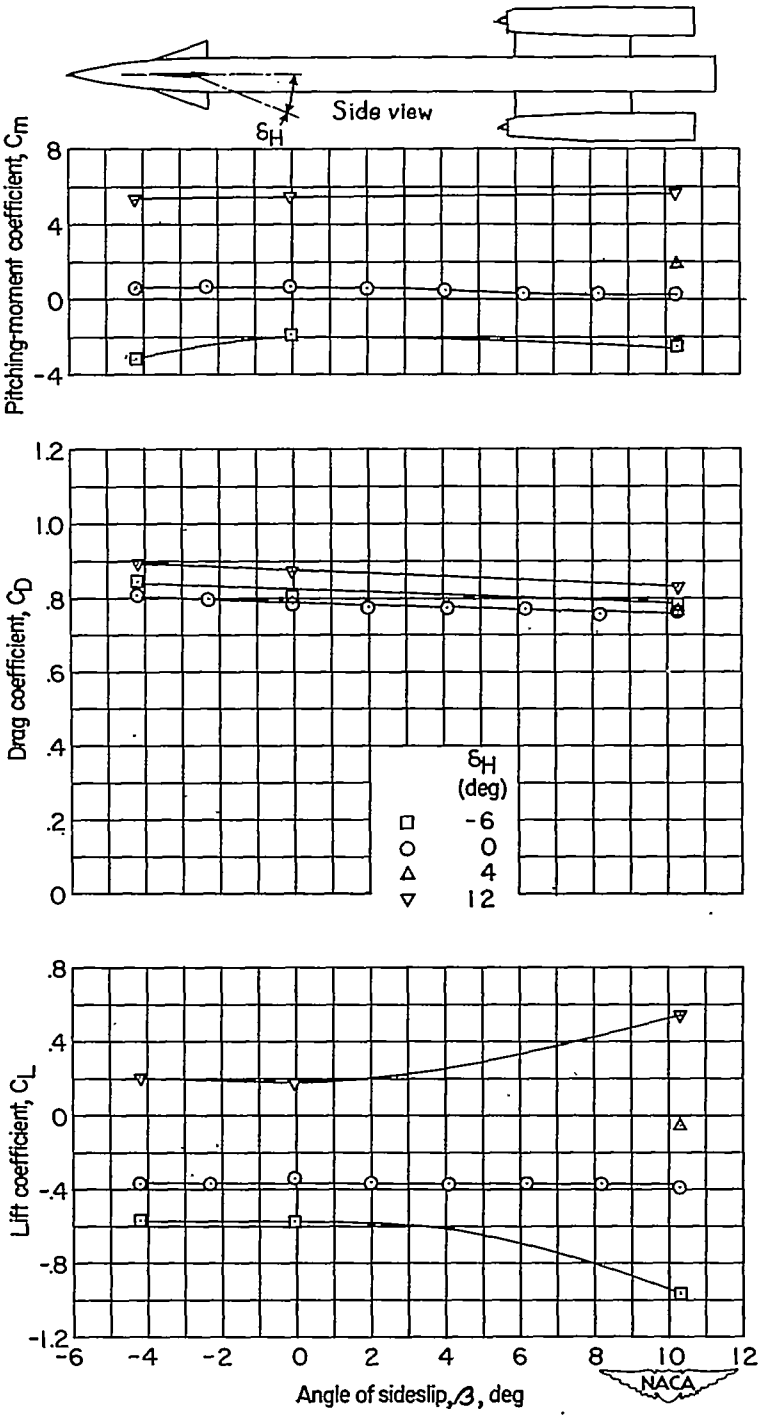

(a) $\delta_V = 6^\circ$.

Figure 9.- Aerodynamic characteristics in sideslip with various control deflections for body with horizontal canard, vertical canard, and nacelles.

[redacted]

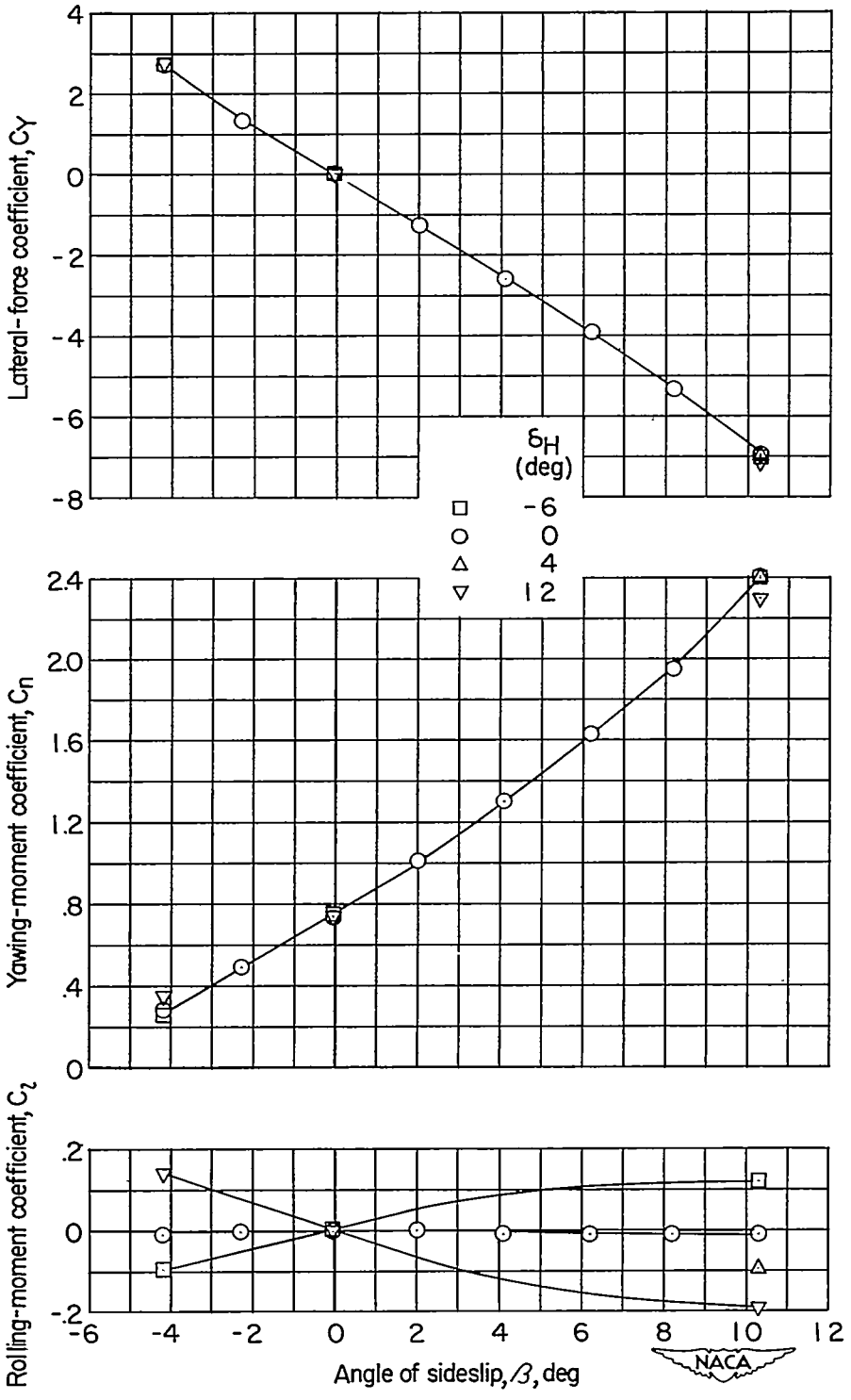

(a) $\delta_V = 6^\circ$. Concluded.

Figure 9.- Continued.

CONFIDENTIAL

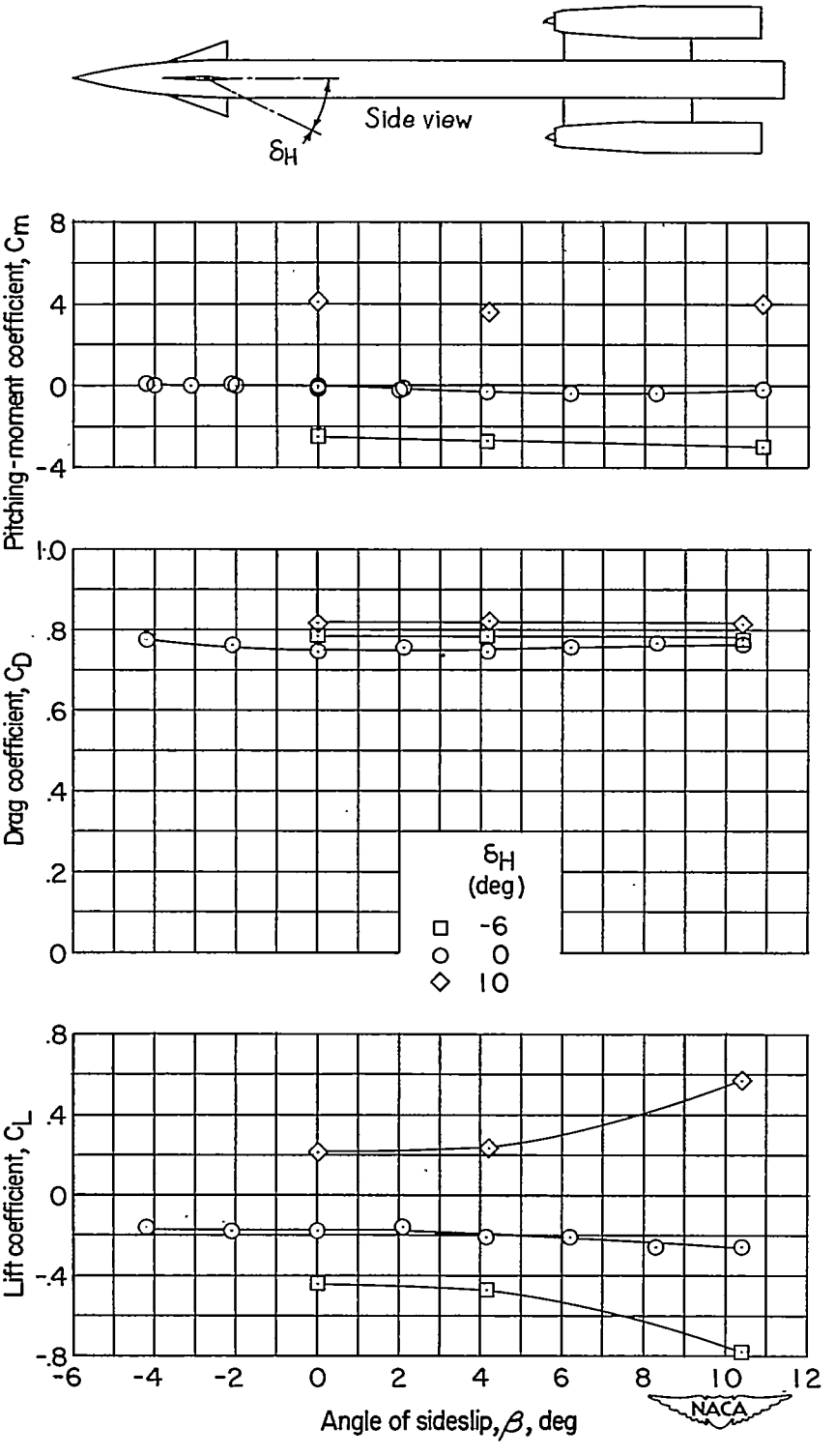

(b) $\delta_V = 0^\circ$.

Figure 9.- Continued.

[redacted]

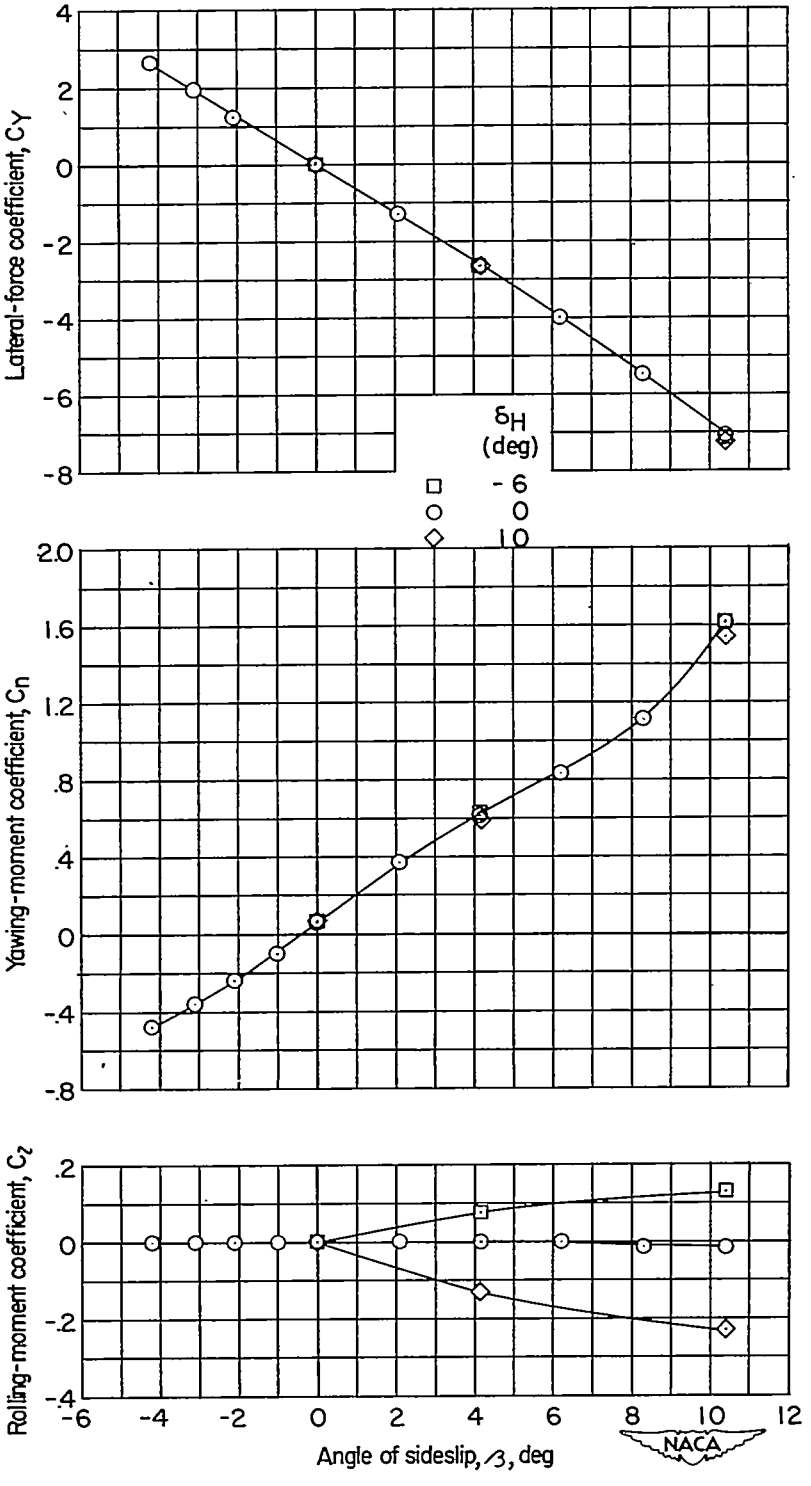

(b) $\delta_V = 0^\circ$. Concluded.

Figure 9.- Concluded.

[redacted]

NACA-Langley - 10-9-53 - 325